
23 High Sliding Velocity Nanotribological Investigations of Materials for Nanotechnology Applications

Nikhil S. Tambe · Bharat Bhushan

Abstract. The advent of microstructures/nanostructures and the subsequent miniaturization of moving components for various nanotechnology applications, such as microelectromechanical/nanoelectromechanical systems, have given paramount importance to the tribology and mechanics on the nanoscale. Most of these microdevices/nanodevices and components operate at very high sliding velocities (of the order of tens of millimeters per second to a few meters per second). Research conducted on various materials, coatings and lubricants has revealed a strong velocity dependence of friction and adhesion on the nanoscale. However, these investigations have been rendered inadequate owing to the inherent limitations on the highest sliding velocities achievable with commercial atomic force microscopes (AFM) that allow the study of nanoscale phenomena. The development of a new AFM-based technique has enabled high sliding velocities that are of engineering importance to be reached. By incorporating high speed piezo stages in a commercial AFM it is possible to conduct fundamental studies at sliding velocities of scientific as well as engineering importance. The utility of the technique is demonstrated through the mapping of nanoscale friction and wear as a function of sliding velocities. These maps provide significant understanding of the dominant friction mechanisms as well as the conditions at which they transition and would potentially enable selection of materials, coatings and lubricants during the design of nanotechnology applications.

Key words: High sliding velocity, Nanotribology, Nanofriction mapping, Nanowear mapping

23.1

Bridging Science and Engineering for Nanotribological Investigations

Nanotechnology, defined literally as any technology performed on a nanoscale that has applications in the real world (Feynman 1960), has spurred the development of innovative microsystems/nanosystems with the discovery of novel materials, processes and phenomena on the microscale/nanoscale and has led to the rapid advancement of microelectromechanical/nanoelectromechanical systems (MEMS/NEMS) and their various biological and biomedical applications, BioMEMS. Recent years have seen a multitude of new emerging applications in this field. Commercial applications such as the microfluidic devices that can manipulate tiny amounts of fluids, “lab-on-chip” sensors used for drug delivery, accelerometers used for automobile air bag deployment and digital micromirror devices used in high-definition TVs and video projectors in homes and theaters are just the tip of the iceberg. In fact these MEMS/NEMS are now believed to be the next logical step in the “silicon revolution.” Visionaries and leading scientists and researchers, presenting at the National Nanotechnology Initiatives workshop on nanotechnology in space exploration held

in Palo Alto, CA, USA in August 2004, have slated the emerging field of nanotechnology to be the next disruptive technology that will have major impact in the next one to three decades. It is estimated that the annual global impact of products where nanotechnology will play a key role will exceed US \$1 trillion by 2015 and would require about two million nanotechnology workers (Roco 2003).

23.1.1

Microtribology/Nanotribology

Despite the increasing popularity and technological advances in MEMS/NEMS applications the severe tribological (friction and wear) problems tend to undermine their performance and reliability. In fact, several studies have shown that the tribology and mechanics of these devices are the limiting factors to the imminent broad-based impact of nanotechnology on our everyday lives (Komvopoulos 2003; Maboudian and Howe 1997; Bhushan 1998, 2003, 2004). Miniaturization and the subsequent development of MEMS/NEMS require better tribological performance of the system components and a fundamental understanding of basic phenomena underlying friction, wear and lubrication on the microscale and the nanoscale (Bhushan 1997, 1998, 1999a,b, 2001a,b, 2004). The components used in microstructures/nanostructures are very light (on the order of a few micrograms) and operate under very light loads (on the order of a few micrograms to a few milligrams). Going from the macroscale to the microscale the surface area to volume ratio increases considerably and becomes a cause of serious concern from the tribological point of view. On microscales, surface forces such as friction, adhesion, meniscus forces, viscous drag and surface tension that are proportional to area significantly increase and limit the life and reliability of MEMS/NEMS. As a result, friction and wear (on the nanoscale) of lightly loaded microstructures/nanostructures are highly dependent on the surface interactions.

The emergence of the new field of microtribology/nanotribology, which pertains to the experimental and theoretical investigations of interfacial processes occurring during adhesion, friction, wear and thin-film lubrication of sliding surfaces on scales ranging from the atomic and molecular scale to the microscale, and its associated techniques (Bhushan 1999a) have provided a viable means of addressing the tribological issues on microscales/nanoscales. Microtribological/nanotribological investigations can be performed using the surface force apparatus (SFA) and the atomic force microscope (AFM) and have already provided valuable insights into the behavior of materials on the nanoscale (Bhushan et al. 1995; Bhushan 1999a). A sharp tip of the AFM developed by Binnig et al. (1986), sliding on a surface simulates microscale/nanoscale contacts, thus allowing high-resolution measurements of surface interactions.

23.1.2

Historical Perspective for Velocity Dependence of Friction

Controlling friction and wear is important in all machine components requiring relative motion. Two basic laws of dry (or conventional) friction are generally obeyed

over a wide range of applications. These laws are often referred to as Amontons's laws, after the French physicist Guillaume Amontons (1699) who rediscovered them in 1699; after Leonardo Da Vinci first described them some 200 years earlier. Amontons's first law states that the friction force is proportional to the normal load. The second law states that friction force (or coefficient of friction) is independent of the apparent area of contact between the contacting bodies. To these two laws, a third law is sometimes added which is often attributed to Coulomb (1785). It states that the kinetic friction force (or coefficient of friction) is independent of the sliding velocity once motion starts. Coulomb also made a clear distinction between static and kinetic friction. These laws have over the years been found to not hold in many cases (Bowden and Tabor 1950, 1964; Moore 1972; Singer and Pollock 1992; Bhushan 1999b), particularly as dimensions of the components and loads used have continued to decrease, tribological and mechanical properties on the microscale to nanoscale have become very important. Various studies on the microscale/nanoscale have indicated a strong normal load and sliding velocity dependence of friction force (Koinkar and Bhushan 1996; Bhushan and Kulkarni 1996; Bouhacina et al. 1997; Baumberger et al. 1999; Riedo et al. 2003; Liu and Bhushan 2002, 2003a,b; Gnecco et al. 2004; Tambe and Bhushan 2004, 2005a–i). Friction on the atomic scale was first reported by Mate et al. (1987). Investigators have subsequently shown that stick–slip on the atomic scale is the result of the energy barrier that needs to be overcome to jump over atomic corrugations on the sample surface and this stick–slip has been theoretically modeled with classical mechanical models (Tomlinson 1929; Tomanek et al. 1991). Further, the potential barrier required to make jumps during stick–slip follows the logarithm of the sliding velocity (Bouhacina et al. 1997; Hoshi et al. 2000; Riedo et al. 2003; Gnecco et al. 2004). Riedo et al. (2002) investigated the kinetics of capillary condensation in nanoscale sliding friction. A logarithmic dependence of friction force on the scan velocity was reported and it was found that while for partially hydrophilic and nanoscale rough surfaces friction decreased logarithmically, for partially hydrophobic surfaces nanoscale friction increased with velocity. The velocity dependence studied was explained with the help of a model based on the kinetics of capillary condensation.

23.2

Need for Speed: Extending the AFM Capabilities for High Sliding Velocity Studies

Extensive as the research efforts have been to characterize and understand the velocity dependence of friction (Fig. 23.1), inherent instrument limitations on the highest sliding velocities achievable with the commercial AFM (less than 100 $\mu\text{m/s}$) (Tambe and Bhushan 2005a) have stymied research pursuits geared towards obtaining a fundamental understanding of failures resulting from high relative sliding velocities found in many real-world applications (tens of millimeters per second to a few meters per second). Many MEMS/NEMS devices (some examples are shown in Fig. 23.2) are designed to operate at very high rotational speeds, ranging from well above 100,000 rpm as in the case of micromotors (Bhushan 2004) to well above

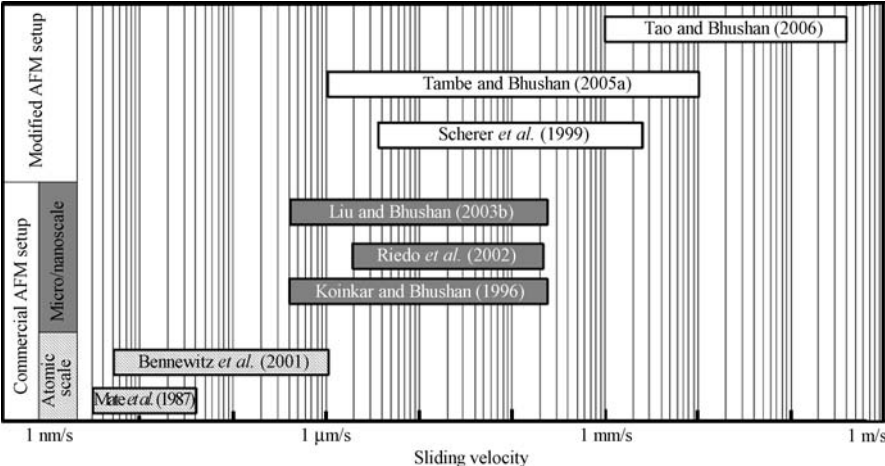


Fig. 23.1. Brief summary of research efforts to study the velocity dependence of friction from atomic scale to microscale/nanoscale over a range of sliding velocities. (AFM atomic force microscope)

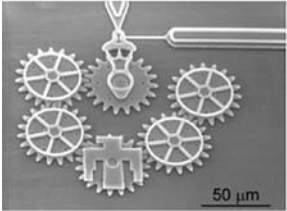
Fig. 23.2. Examples of nanotechnology devices that operate at high sliding velocities: electrostatic micromotor (Tai et al. 1989), microturbine (Spearing and Chen 1997), microgear drive (<http://www.sandia.gov>) and planetary gear system (Lehr et al. 1996)



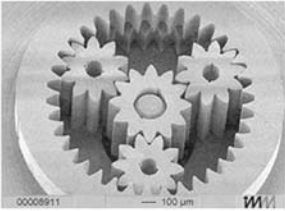
Electrostatic micromotor (Tai et al., 1989)



Microturbine bladed rotor and nozzle guide vanes on the stator (Spearing and Chen, 2001)



Six-gear chain (www.sandia.gov)



Ni-Fe wolfram-type gear system by LIGA (Lehr et al., 1996)

1,000,000 rpm for microgas turbines (Frechette et al. 2005). Given the size of these devices (the micromotor has a rotor diameter of 120 μm), the relative sliding velocities that they operate at can reach several meters per second. With the lack of sufficient experimental evidence, theoretical formulations have remained limited (Riedo et al. 2002; Tambe 2005). A study to investigate the velocity dependence of friction, adhesion and wear for sliding velocity ranges of engineering importance would be crucial to the future design and development of microstructures/nanostructures and devices for various nanotechnology applications.

23.2.1

Modifications to the Commercial AFM Setup

There are a number of commercial AFMs that have been available on the market since 1989. Depending on the design of the AFM, i.e., whether the cantilever tip is scanned or the sample is scanned, AFMs can be broadly classified as large-sample and small-sample AFMs, respectively (Bhushan 1999a). Since the tip is held stationary in the small-sample AFM, it provides better resolution and there is less noise contamination of the measured data, particularly for small scan sizes. However, a small-sample AFM, as the name suggests, inherently requires the sample studied to be of small size and weight; otherwise the piezo scanner operation is hindered. A large-sample AFM provides the capability of studying larger samples and also provides the added flexibility needed for mounting samples on custom-built stages for performing a wide array of studies. To achieve higher sliding velocities between the AFM cantilever tip and the sample surface, the primary approach has been to incorporate a customized stage, capable of providing high sliding velocity, into the commercial AFM setup. To date various techniques have been developed that modify the basic AFM setup in order to enhance its measurement capabilities and broaden the scope of tribological studies into higher sliding velocity regimes. One approach has been to mount samples on a shear wave transducer and then drive the transducer at very high frequencies (in the megahertz range) (Yamanaka and Tomita 1995; Scherer et al. 1999; Marti and Krottil 2001; Reinstadtler et al. 2003). In this manner, velocities on the order of a few millimeters per second can be achieved. In techniques employed by researchers using a shear wave transducer, the modulation amplitude, however, remains very small, in the nanometer range. Moreover friction force measurements as made by these researchers do not directly provide a fundamental understanding of nanoscale friction since they use a combination of oscillators, one to achieve high velocity and another for scanning. This does not provide a good estimate for nanoscale friction resulting from actual relative sliding between two components as oscillation of the tip (or the sample) while scanning changes the adhesive force at the tip-sample interface and influences stick-slip behavior. The main challenges while modifying the AFM setup to achieve higher velocities are maintaining a constant velocity profile during the entire scan duration and at the same time scanning on larger surface areas to get a better understanding of nanotribological properties.

An alternative approach for accomplishing such a modification is using either a motorized stage or a piezo stage with large amplitude (approximately 100 μm) and relatively low resonance frequency (a few kilohertz). The most important parameters that need to be taken into consideration before implementing such modifications are the maximum travel (or scan size), the resolution, the accuracy and repeatability (hysteresis in forward and reverse scans), a constant velocity requirement over the entire scanning length, and the maximum sample size and weight allowable (this is particularly important for piezo stages). Motorized stages can prove to be relatively inferior to piezo stages owing to vibration-related issues, particularly in the direction perpendicular to the scanning axis (along the normal load axis of the cantilever tip). Such a stage can result in the cantilever tip being subjected to a constant change in normal load and the “chatter” can contaminate measurements. Piezo stages provide better performance in this respect. However, the disadvantage in using piezo stages

is that they can be limited by the maximum travel, the scanning frequency and the sample size. To achieve high velocities (in the tens of millimeters per second range and beyond) using a piezo stage implies that both the scanning frequency and the scan size should be relatively high. In most instances, however, there is a trade-off between the maximum travel and the frequency of the piezo stage. Piezo stages can introduce mechanical noise as a result of “ringing” which occurs because of poor piezo tracking. Open loop operation (i.e., no active feedback) can result in the piezo losing its tracking accuracy at high frequencies and thus the requirement of having a constant velocity over the entire scan length is not met. Instead, therefore, a closed loop operational mode can be employed; however, this is generally at the expense of the maximum travel distance (scan size) achievable.

We discuss two approaches as developed by Tambe and Bhushan (2005a) and Tao and Bhushan (2006, 2007). They incorporate custom-calibrated piezo stages into a commercial AFM setup.

23.2.1.1
Large Amplitude Piezo Stage

Tambe and Bhushan (2005a) modified a commercial AFM setup (D3100, Nanoscope IIIa controller, Digital Instruments, Santa Barbara, CA, USA) by incorporating a custom-calibrated piezo stage (P621.1CL, HERA Nanopositioner with capacitive feedback, Polytec PI, Karlsruhe, Germany). This piezo stage has an unloaded resonance frequency of 800 Hz and a maximum scan length of 100 μm. The piezo stage drive units are based on P-885 PICMA® low-voltage multilayer piezo ceramics, having an extremely stiff friction-free flexure system with excellent guiding accuracy (small tilt angles over the entire travel range). This design dispenses ultrahigh power electronics that can cause conventional piezo stacks to heat excessively when operated at high frequencies (D. Rego, personal communication 2003). Table 23.1 lists specifications of the piezo stage.

In the modified setup, the single-axis piezo stage is oriented such that the scanning axis is perpendicular to the long axis of the AFM cantilever (this corresponds to the 90° scan angle mode of the commercial AFM). Scanning is achieved by providing a triangular voltage pulse to the piezo amplifier. Figure 23.3a shows a schematic of the experimental setup and a cross-sectional schematic of the piezo stage. The piezo crystal drives the flexure and the sample mounted on top of it at the desired frequency, corresponding to the input voltage pulse. The displacement is monitored using an integrated capacitive feedback sensor, located diametrically opposite to the piezo crystal as shown in Fig. 23.3a. The capacitive sensor has a stationary

Table 23.1. Specifications of the P621.1CL piezo stage

Closed loop travel	100 μm	Tilt (perpendicular to scan axis)	3 μrad
Closed loop linearity	0.01%	Electrical capacitance	1.5 μF (±20%)
Stiffness	0.35 N/μm	Unloaded resonance frequency	800 Hz (±20%)
Maximum load	10 N	Resonance frequency at 20g	520 Hz (±20%)
Lateral force limit	10 N	Operating temperature range	−40 to 120 °C

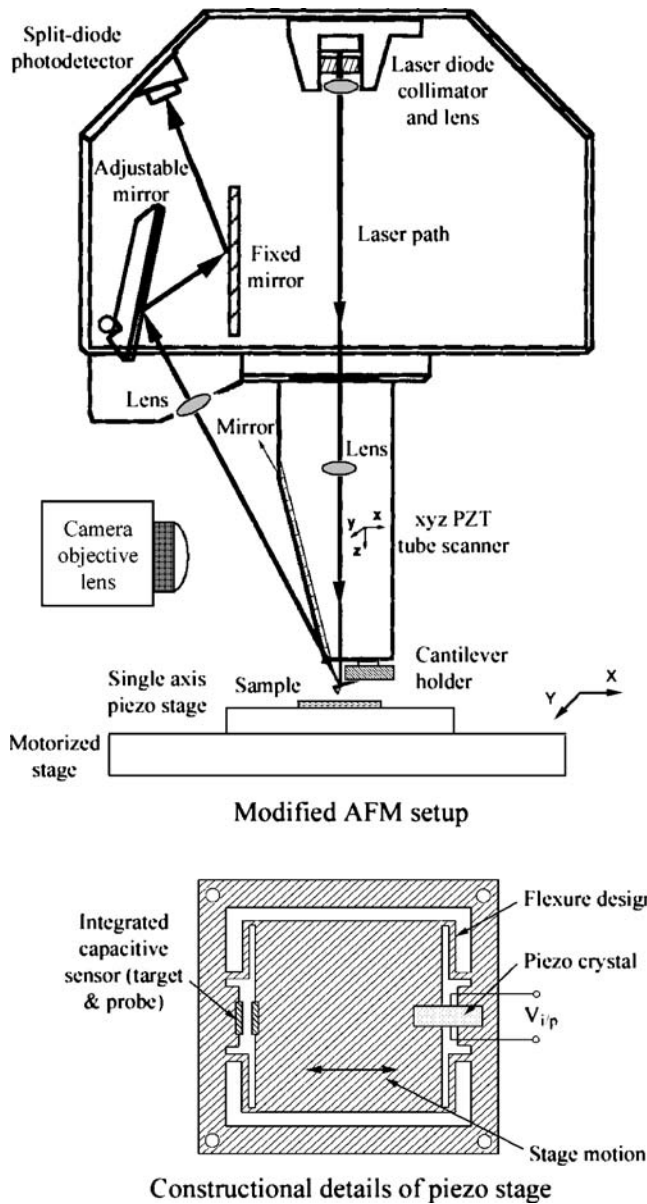


Fig. 23.3. a Modifications made in the commercial AFM setup using the single-axis piezo stage and a cross-sectional view showing construction details of the piezo stage. The integrated capacitive sensors are used as feedback sensors to drive the piezo. The piezo stage is mounted on the standard motorized AFM base and is operated using independent amplifier and controller units driven by a frequency generator (not shown)

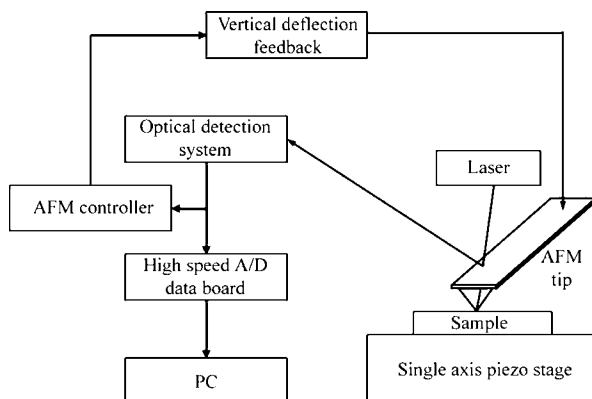


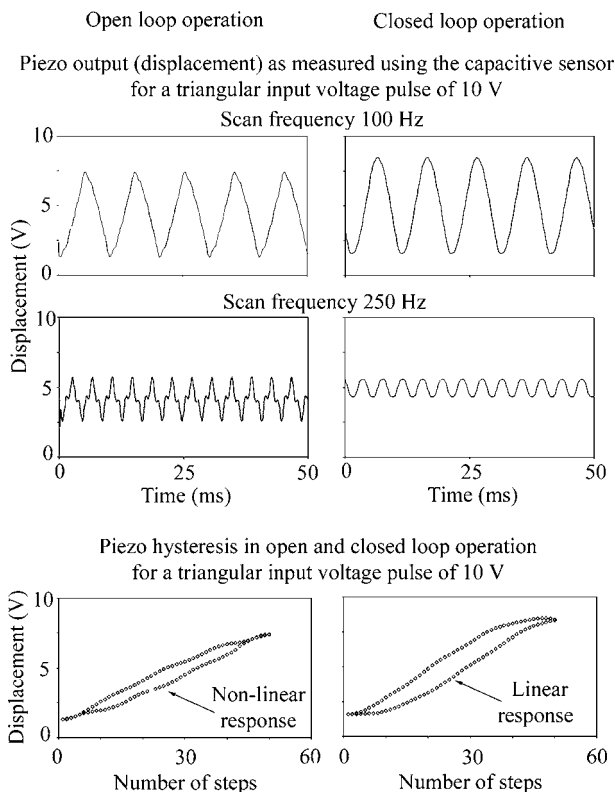
Fig. 23.3. b Operational flowchart showing the various components of stage operation. (From Tambe and Bhushan 2005a)

target element mounted on the stage block and a moving probe element mounted on the flexure. The capacitance change, corresponding to the stage displacement, gives an indication of the amount of displacement. The stage can be operated in both open loop and closed loop operational modes. In the closed loop mode, the capacitive sensor signals are used as feedback by the piezo controller to provide better guiding and tracking accuracy. The closed loop position control of piezoelectric-driven stages using capacitive feedback sensors provides linearity of motion better than 0.01% with nanometer resolution and a stable drift free motion (Anonymous 2003).¹ Figure 23.3b shows an operational flowchart for the piezo stage. For scanning purposes, a triangular voltage pulse with 0–10-V maximum peak-to-peak voltage is input to the piezo amplifier using a function generator. The triangular pulse gives constant displacement with respect to time and thereby ensures a constant scanning velocity, which is necessary during friction measurements. The input voltage pulse is fed into the piezo amplifier and controller circuit, where it was amplified to 0–100-V range and used for driving the piezo crystal. The piezo displacement is monitored by the capacitive sensor and in closed loop operational mode is fed back to the controller.

The piezo stage displacements as measured by the capacitive sensors at two high frequencies in open and closed loop modes of operation are shown in Fig. 23.4. The open loop mode of operation (i.e., when no feedback was employed) had the advantage that piezo tracking was much better during the reversals in the direction of the stage motion while scanning, as seen in Fig. 23.4. However, in the absence of active tracking, the piezo displacements stray away considerably from the input triangular profile. This is particularly evident at 250-Hz scan frequency when piezo

¹ The piezo stage drive units, based on P-885 PICMA® low-voltage multilayer piezo ceramics, have an extremely stiff friction-free flexure system with excellent guiding accuracy (typically less than 5 μ rad pitch/yaw over the entire travel range). The closed loop position control of piezoelectric-driven stages using capacitive feedback sensors provides linearity of motion better than 0.01% with nanometer resolution and a stable drift-free and hysteresis-free motion.

Fig. 23.4. Piezo stage displacements (in volts) as measured using the capacitive sensor for open loop and closed loop operation at 100- and 250-Hz scanning frequencies; and piezo hysteresis under open and closed loop operational modes at 100-Hz scan frequency. (From Tambe and Bhushan 2005a)



“ringing”, high-frequency noise, becomes a significant factor. The capacitive sensor can be used for providing feedback to the piezo controller and this improves the piezo tracking considerably. In this case, the stage reversals are not linear and so stage velocity is not constant towards the ends when the stage reverses direction. However, the tracking is significantly improved as a result of the active feedback loop and this ensures that the velocity remains constant over most of the stage travel. Nonetheless the piezo does show hysteretic behavior for a 100-Hz scan frequency (Fig. 23.4). Hysteresis (area enclosed by the curve) is higher in the closed loop operational mode, but this mode also gives a linear response over a large portion of the total scan length. The linear response implies a constant velocity and hence is more useful for friction force measurements. The commercial AFM setup modified with this custom-calibrated nanopositioning stage is capable of achieving high sliding velocities up to 10 mm/s.

The output of the capacitive sensor was calibrated to get the actual scan size in microns. A capacitive sensor output voltage of 1 V corresponds to a scan size of 10 μm . This calibration data were obtained from the stage manufacturer (Physik Instrumente, Karlsruhe, Germany). Figure 23.5 shows the calibration chart for the piezo stage over a large range of scanning frequencies from 1 to 500 Hz and for scan sizes of 0–25 μm . The chart was obtained by running the stage in closed loop operational mode and monitoring the capacitive sensor signals for different

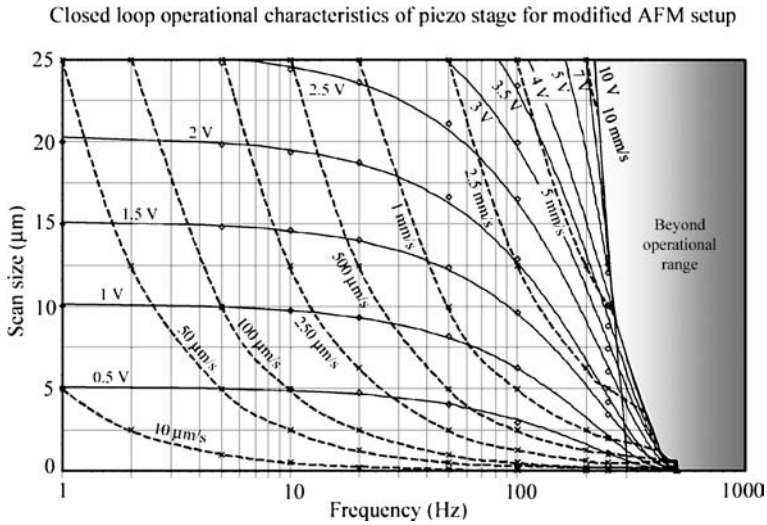


Fig. 23.5. Calibration chart for the piezo stage giving scan sizes over a range of operating voltages (0–10 V) and frequencies (1–500 Hz) for the closed loop operational mode. *Solid lines* and *dashed lines* correspond to constant input voltage and constant velocity, respectively. (From Tambe and Bhushan 2005a)

input voltage pulses. Constant input voltage lines (solid lines) indicate that the stage performance is that of a critically damped system. The constant velocity lines (dashed lines) indicate the range of sliding velocities achievable with the modified AFM setup. The maximum input voltage to drive the piezo is 10 V and the shaded area on the calibration chart indicates a region that was beyond the operational limit of the piezo stage. It should be noted that the stage has a maximum scan length of 100 μm. On the basis of the calibration chart, the input voltage pulse can be selected in order to obtain a specific scan size at a given scanning frequency or for determining the scanning frequency necessary at a given scan size to achieve the required scanning velocity.

23.2.1.2
Ultrasonic Linear Piezo Drive

Tao and Bhushan (2006, 2007) have developed another piezo-based technique for achieving sliding velocities up to 200 mm/s. The system includes a custom-calibrated piezo stage or a piezo ultrasonic linear drive (M663.465, Physik Instrumente), a stage controller (C865, Physik Instrumente), and a custom-designed software application for operation control (Fig. 23.6a,b). The control application sends motion parameters to the controller, and the controller calculates the exact position of each step and sends the position signal to the stage.

The piezo stage has a maximum scan length of 19 mm and a maximum velocity of 400 mm/s. Table 23.2 lists specifications of the stage. The key part of the stage, shown in Fig. 23.6a, is a rectangular monolithic piezoceramic plate (the stator) with

Applied Scanning Probe Methods IX
Characterization

Bhushan, B.; Fuchs, H.; Tomitori, M. (Eds.)

2008, LIX, 387 p., Hardcover

ISBN: 978-3-540-74082-7